Diode-pumped orthogonally polarized Nd:$LuVO_4$ lasers based on the $^4F_{3/2}$–$^4I_{11/2}$ transition

Yanfei Lü,[1,*] Jing Xia,[1] Xihong Fu,[2] Anfeng Zhang,[3] Huilong Liu,[1] and Jing Zhang[1]

[1]*School of Science, Changchun University of Science and Technology, Changchun 130022, China*
[2]*State Key Laboratory of Luminescence and Applications, Changchun Institute of Optics, Fine Mechanics and Physics, Chinese Academy of Sciences, Changchun 130033, China*
[3]*Laboratory of Info-integration Technology, Xi'an Institute of Applied Optics, Xi'an 710065, China*
**Corresponding author: optik@sina.com*

Received January 29, 2014; revised February 23, 2014; accepted February 24, 2014;
posted February 26, 2014 (Doc. ID 205669); published March 28, 2014

A diode-pumped simultaneous orthogonally polarized continuous-wave (cw) dual-wavelength Nd:$LuVO_4$ laser based on the $^4F_{3/2}$ – $^4I_{11/2}$ transition is experimentally demonstrated. A theoretical analysis has been introduced to determine the threshold conditions for simultaneous orthogonally polarized dual-wavelength laser. Using a polarization beam splitter included resonant cavity in the experiments, simultaneous orthogonal polarized dual-wavelength Nd:$LuVO_4$ laser operation was realized at two close wavelengths near 1060–1070 nm. To our knowledge, this is the first work of realizing simultaneous dual-wavelength Nd:$LuVO_4$ laser operation near 1060–1070 nm.

OCIS codes: (140.3480) Lasers, diode-pumped; (140.3580) Lasers, solid-state; (140.3410) Laser resonators.
http://dx.doi.org/10.1364/JOSAB.31.000898

1. INTRODUCTION

Simultaneous dual-wavelength laser from a single laser medium is of fundamental scientific interest and has applications in various practical fields, such as holographic interferometry [1], medical treatment [2], lidar [3], nonlinear optical mixer [4], and precision laser spectroscopy [5]. After Bethea first introduced dual-wavelength Nd:YAG laser in 1987 [6], dual-wavelength lasers based on Nd:YAG [7–11], Nd:YLF [12], Nd:YVO_4 [13–17], Nd:$GdVO_4$ [18–22], Nd:$LuVO_4$ [23], Nd:YAP [24,25], Nd:$LuYSiO_5$ [26], Nd:Lu_2SiO_5 [27], and Nd:$Sc_{0.2}Y_{0.8}SiO_5$ [28] have been reported. In the dual-wavelength lasers, the dual-wavelength lasers with orthogonal polarizations are new attractive devices for various applications, such as laser interferometry and precision metrology [29,30], especially in precision measurement including the precision measuring of length, displacement, angle, velocity, pressure, magnetic field, and so on [31–34]. The laser media are one of the most important parts of simultaneous dual-wavelength solid-state lasers. Nd-doped laser crystals, because of their high gains and the good thermal and mechanical properties, are by far the most important laser media. Vanadate crystals have become one category of the most important host materials for the Nd ion, which provides the most efficient laser media. Nd-doped vanadate crystals possessing many sharp fluorescent lines, especially in the $^4F_{3/2}$ – $^4I_{11/2}$ transition, are natural candidates to realize the dual-wavelength solid-state lasers. A well-known representative is Nd:YVO_4, which has been widely used both in research and commercial devices. Another vanadate crystal, Nd:$GdVO_4$, which was confirmed to be superior to Nd:YVO_4 in thermal properties, was also investigated extensively. Yet another member from the vanadate family, Nd:$LuVO_4$, has attracted much attention because it has larger absorption and emission cross sections than Nd:YVO_4 and Nd:$GdVO_4$ [35].

Recently, Nd:YVO_4 and Nd:$GdVO_4$ lasers based on the $^4F_{3/2}$ – $^4I_{11/2}$ transition have been demonstrated for achieving dual-wavelength emission with orthogonal polarizations, in which two a-cut YVO_4/Nd:YVO_4 crystals with their c axis orthogonally [17] or a polarization beam splitter (PBS) [20] was employed. Figure 1 displays the room-temperature polarized fluorescence spectrum of the Nd:$LuVO_4$ crystal for the $^4F_{3/2}$ – $^4I_{11/2}$ laser transition. As shown in Fig. 1, the emission lines of Nd:$LuVO_4$ are typically near 1060–1070 nm. The strongest emission line of Nd:$LuVO_4$ is typically 1066 nm in π-polarization ($E//c$). Comparing with this line, the emission lines of 1062, 1065, and 1068 nm in σ-polarization ($E\perp c$) are medium strong. However, because the gain of 1066 nm in π-polarization (emission cross section $\sigma = 146 \times 10^{-20}\,\mathrm{cm}^2$) is almost 5 times higher than that of 1062 nm ($\sigma = 25.4 \times 10^{-20}\,\mathrm{cm}^2$), 1065 nm ($\sigma = 20 \times 10^{-20}\,\mathrm{cm}^2$), and 1068 nm ($\sigma = 36.4 \times 10^{-20}\,\mathrm{cm}^2$) in σ-polarization, the σ-polarization emission is normally depressed by the π-polarization emission of 1066 nm if no specific measure is applied to control the gain competition in the laser cavity. It is also seen that the emission spectra of Nd:$LuVO_4$ crystals in the range of 1080–1090 nm display comparable radiation strengths in π- and σ- polarizations. More recently, a dual-wavelength Nd:$LuVO_4$ laser with orthogonal polarizations in the range of 1080–1090 nm has been experimentally demonstrated [23]. However, to our knowledge, no work on the simultaneous orthogonally polarized dual-wavelength Nd:$LuVO_4$ laser operation near 1060–1070 nm has been reported. The main reason is that dual-wavelength operation with the same laser medium is rather difficult because of the strong gain competition between the two polarizations.

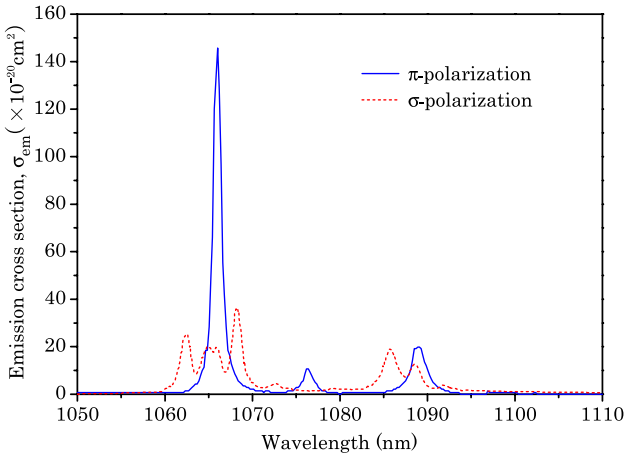

Fig. 1. Room-temperature polarized emission spectra for the $^4F_{3/2} - {}^4I_{11/2}$ laser transition in the Nd:$LuVO_4$ crystals [35].

However, such a dual-wavelength laser would be especially valuable as a compact and strong laser source to generate the terahertz emission because the frequency difference [36] between two polarizations is about 0.5 THz. Coherent terahertz waves, traditionally defined in the frequency range of 0.1–3 THz, have great potential for terahertz imaging, sensing, and terahertz spectroscopy applications [37–39].

In this paper, we will present our recent results of exploring a simultaneous dual-wavelength Nd:$LuVO_4$ laser. The condition of gain-to-loss balance for achieving the orthogonally polarized dual-wavelength operation was theoretically analyzed. By separating the orthogonal polarized beams with a PBS and then controlling the cavity loss of π-polarization, simultaneous dual-wavelength Nd:$LuVO_4$ laser operation was experimentally realized at two close wavelengths near 1060–1070 nm.

2. EXPERIMENTAL SETUP AND THEORETICAL ANALYSIS

The experimental setup used is described in Fig. 2. The optical pumping was done by using fiber-coupled (diameter of 400 μm and numerical aperture NA = 0.22) diode lasers from Coherent Co., USA. The 809 nm emitting diode output 20 W of pump power with an emission bandwidth of 2.0 nm (FWHM definition). The coupling optics consists of two identical plano–convex lenses with focal lengths of 15 mm used to reimage the pump beam into the laser crystal at a ratio of 1:1. The coupling efficiency is 95%. The gain medium was a 0.5 at. % Nd:$LuVO_4$ crystal with a length of 5 mm cut along the a axis. The Nd:$LuVO_4$ crystal was wrapped with indium foil and mounted at a thermal electronic cooled (TEC) copper block, and the temperature was maintained at 20°C. The whole cavity was also cooled by TEC. Both sides of the Nd:$LuVO_4$ were

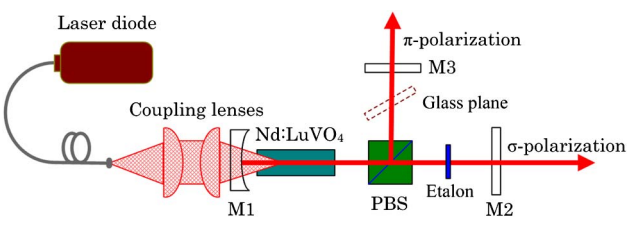

Fig. 2. Experimental setup for the diode-pumped orthogonally polarized dual-wavelength Nd:$LuVO_4$ laser.

coated for high transmission (HT) from 1060 to 1070 nm. A PBS was placed in the cavity to split the beams polarizing in two orthogonal directions. The concave mirror, M1, with a radius of curvature −100 cm was used as the input coupler, which was coated for high reflectivity from 1060 to 1070 nm and HT at 809 nm. The plane mirror, M2, was used as the output coupler for the mode with horizontal polarization. Another plane mirror, M3, was used as the output coupler for the mode with vertical polarization. To select the lasing wavelength, we inserted a 25 μm etalon into the σ-polarized emission cavity.

The dual-wavelength resonator characteristics, i.e., the gain and the loss for each transition, were selected to give similar pump thresholds at both lasing wavelengths. In previous works dual-wavelength emission was obtained by employing linear resonators with two or three mirrors [13]; the ratio between the sizes of the two laser beams inside the laser crystal was adjusted by changing the resonator's length and mirrors with special coatings for both wavelengths in order to achieve the same threshold condition. For a diode-end-pumped solid-state four-level laser, the threshold condition for each transition can be written as [21,40]

$$P_{\mathrm{th},i} = \frac{\ln(1/R_i) + L_i}{2\eta_i f_i \sigma_i \tau} \frac{\pi h\nu_p \omega_p^2}{1 - \exp(-2\omega_p^2/\omega_i^2)} \quad i = 1, 2, \tag{1}$$

where R_i is the reflectivity of the output mirror, L_i is the round-trip cavity excess losses at the corresponding transition wavelength, η_i is the quantum efficiency, f_i is the population number in the Stark components of the upper laser levels, $h\nu_p$ is the pump photon energy, σ_i is the emission cross section, τ is the fluorescence lifetime, ω_p is the pump beam waist in the active medium, ω_i the laser beam waist. Here, $i = 1$, 2 represents the two wavelengths of σ-polarization and π-polarization, respectively.

From Eq. (1), the ratio of laser thresholds γ for two wavelengths of π-polarization and σ-polarization can be expressed as

$$\gamma = \frac{P_{\mathrm{th},2}}{P_{\mathrm{th},1}} = \frac{\ln(1/R_2) + L_2}{\ln(1/R_1) + L_1} \frac{\eta_1 f_1 \sigma_1}{\eta_2 f_2 \sigma_2} \frac{1 - \exp(-2\omega_p^2/\omega_1^2)}{1 - \exp(-2\omega_p^2/\omega_2^2)}. \tag{2}$$

For obtaining a dual-wavelength operation, needs to be introduced to reach the condition of $\gamma \geq 1$. For example, for achieving the orthogonally polarized laser at 1068 and 1066 nm, with Eq. (2) and the parameters in the experiment: $\eta_1 = \eta_2$, $f_1 = 0.46$, $f_2 = 0.54$, $L_1 \approx L_2 \approx 0.01$, $\omega_p \approx 200$ μm, $\omega_1 \approx \omega_2 \approx 100$ μm, $\sigma_1 = 36.2 \times 10^{-20}$ cm^2, and $\sigma_2 = 146 \times 10^{-20}$ cm^2, the condition of $\gamma \geq 1$ would be fulfilled for R_1 value of 94.2% at 1068 nm; the corresponding reflectivity R_2 at 1066 nm should be ≤73.5%. The value of L_i was measured by the Findlay–Clay method [41].

3. RESULTS AND DISCUSSION

First of all, the experiment on single-wavelength Nd:$LuVO_4$ laser operation was performed. The output couplers, M2 and M3, have the transmissions of 5.8% near 1060–1070 nm and 10% around 1066 nm, respectively. Figure 3 presents the dependence of the output power on the incident pump power for the single-wavelength Nd:$LuVO_4$ laser. At 1066 nm a maximum power of 9.1 W was obtained with the pump power of

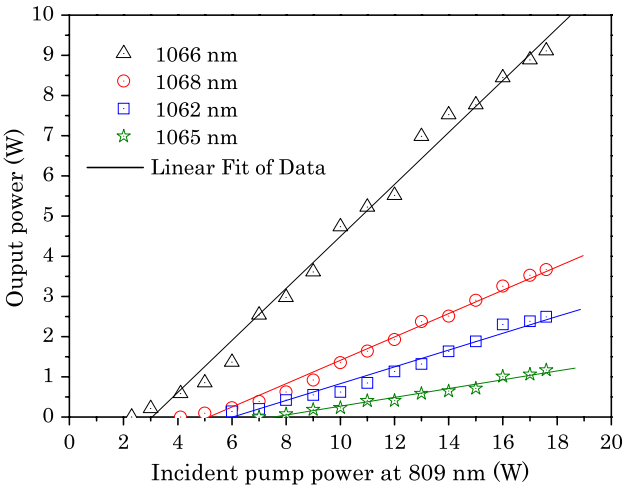

Fig. 3. Output power versus the incident pump power for single-wavelength operation.

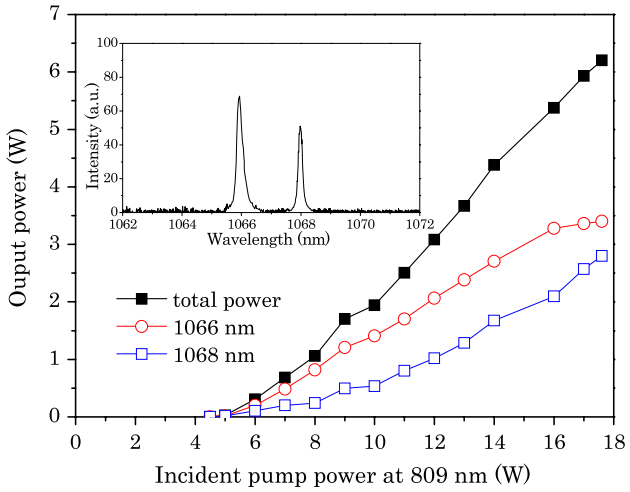

Fig. 4. Dependence of the relative output powers at 1066 and 1068 nm on the incident pump power ($\gamma = 1$). Inset: optical spectrum of dual-wavelength operation at the maximum output power.

17.6 W. The pump threshold and the slope efficiency were 2.3 W and 64.6%, respectively. Because the pump beam quality is bad ($M^2 \approx 400$), in order to get good spatial overlap between pump and laser modes, the ratio of pump and laser beam diameters must be bigger, which leads to a relatively high threshold. We found that the present laser output is linearly polarized along the π-direction. The 1060–1070 nm transition in the σ-polarized direction was suppressed completely due to strong gain competition with the 1066 nm transition in the π-polarized direction. To avoid gain competition in the π-polarized direction, the cw σ-polarized laser operation without the M3 was performed. When the incident pump power was increased to about 4.1 W, the laser oscillation was obtained only at 1068 nm. The maximum output power at 1068 nm of 3.7 W was obtained with a slope efficiency of 29.1%. Laser emission at wavelengths other than 1068 nm can be achieved by rotating the etalon. Thus, lasing oscillation has been demonstrated at 1062 and 1065 nm without line competition. The measured output power varied from 2.5 W at 1062 nm to 1.4 W at 1065 nm. As can be seen from Fig. 3, the thresholds of 1062 and 1065 nm are higher than that of 1068 nm. It is because the emission cross section of 1068 nm is higher than that of both 1062 and 1065 nm.

In order to realize the operation of simultaneous dual-wavelength laser, the cw Nd:$LuVO_4$ laser operation with the two polarized directions was demonstrated and analyzed. According to Eq. (2), if we assumed that the reflectivity for 1068 nm emission was 94.2%, the reflectivity for 1066 nm emission must be 73.5% to satisfy the simultaneous oscillation condition (i.e., $\gamma = 1$) in Nd:$LuVO_4$ laser at 1068 and 1066 nm. The experimental value of reflectivity at 1068 nm and the corresponding value of reflectivity at 1066 nm are 94.2% and 72.8%, respectively. Figure 4 shows results on the simultaneous dual-wavelength emission at 1068 and 1066 nm. The laser threshold was 4.5 W. At an incident pump power of 17.6 W, the maximum output power was 2.8 W at 1068 nm and 3.4 W at 1066 nm. A total output power of 6.2 W was achieved with optical conversion efficiency of 35.2%. The stability testing is carried out by monitoring the output powers of each wavelength with a Field-Master-GS powermeter at 10 Hz. The fluctuations for 1068 and 1066 nm lights at the pump power of 17.6 W are about 2.1% and 2.8% in 4 h, respectively. The M^2 values for 1068 and 1066 nm lights at the pump power of 17.6 W were found to be around 1.14 and 1.19, respectively. Using the LABRAM-UV spectrum analyzer to scan the Nd:$LuVO_4$ dual-wavelength laser and dealing with the data with software, the spectrum of the dual-wavelength laser at the pump power of 17.6 W is shown in the inset of Fig. 4. The central wavelengths are 1068.0 and 1065.9 nm, with the spectral linewidths (FWHM) of 0.31 and 0.42 nm, respectively.

In fact, when $\gamma > 1$, that is to say $P_{th,2} > P_{th,1}$, the dual-wavelength oscillation can be also obtained, but the laser will first emit the radiation at the weaker line at 1068 nm and then emit the radiation at the stronger line at 1066 nm under a higher pump power. In order to reach the condition of $\gamma > 1$, an uncoated glass plate with a thickness of 0.3 mm was inserted in the π-polarized emission cavity. In our experiment, the c axis of Nd:$LuVO_4$ crystal is set to be placed in the vertical direction, which the plane of incidence is in the horizontal direction. As a result, the π-polarized wave is perpendicular to the plane of incidence, corresponding to the s wave. Thus, the reflectivity of the π-polarized emission caused by the Fresnel reflection for the s wave can be given by [42]

$$R(\theta_i) = \left|\frac{\sin(\theta_i - \theta_t)}{\sin(\theta_i + \theta_t)}\right|^2 + \left[1 - \left|\frac{\sin(\theta_i - \theta_t)}{\sin(\theta_i + \theta_t)}\right|^2\right] \cdot \left|\frac{\sin(\theta_t - \theta_i)}{\sin(\theta_t + \theta_i)}\right|^2, \tag{3}$$

where θ_i is the inclined angle of the glass plane (equal to the incident angle of light), θ_t is the refractional angle of light, and $\sin\theta_i = n \sin\theta_t$, $n = 1.5$ is the refractive index of the glass. Therefore, the round-trip reflection loss of the π-polarized emission can be written as

$$L(\theta_i) = R(\theta_i) + [1 - R(\theta_i)]R(\theta_i). \tag{4}$$

With Eqs. (2)–(4) and the parameters in the experiment, the ratio of laser thresholds γ and the round-trip reflection loss of the π-polarized emission $L(\theta_i)$ are calculated as a function of incident angle θ_i, as shown in Fig. 5.

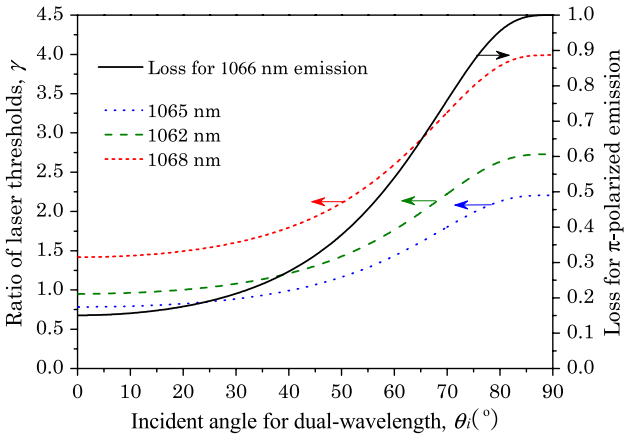

Fig. 5. Dependence of the ratio of laser thresholds and the round-trip reflection loss of π-polarized emission on the incident angle of dual-wavelength, respectively.

We adjusted the incident angle θ_i to around 10°, the ratio of laser thresholds for 1066 and 1068 nm, $\gamma = 1.4$. Figure 6 shows results on the dual-wavelength emission at 1068 and 1066 nm. As can be seen from Fig. 6, when γ was increased to 1.4, the threshold of lasing at 1068 nm decreased to 4.1 W and the output power increased monotonically up to 3.5 W for 17.6 W of pump power. The 1066 nm laser emission started to oscillate at an increased threshold of 5.2 W and reached a maximum output power of 1.7 W at 13 W of pump power, with a strong decrease beyond this pump power. The reason is that in the gain competition between 1068 and 1066 nm lines, with the increasing γ value, the loss of the 1066 nm line increases, which leads to the gain at 1068 nm exceeding that at 1066 nm around 13 W of pump power, thus the output power of 1066 nm decreases and that of 1068 nm increases beyond 13 W of pump power. The beam qualities of the laser beams were observed at different pump powers. The M^2 factor of 1066 nm emission is estimated to be approximately 1.12 near threshold, and then increases to 2.53 at pump power greater than 17.6 W. On the other hand, the 1068 nm emission maintains the beam quality factor M^2 less than 1.17 over the full range of pump powers.

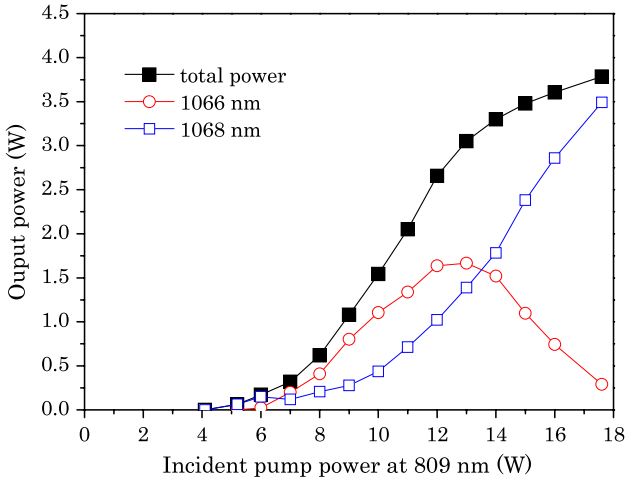

Fig. 6. Dependence of the relative output powers at 1068 and 1066 nm on the incident pump power ($\gamma = 1.4$).

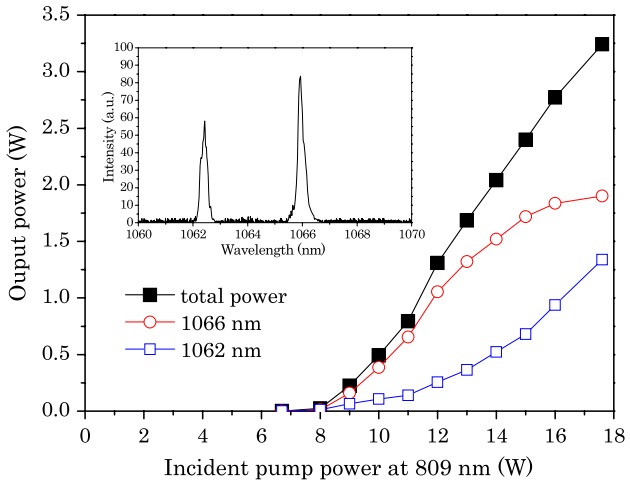

Fig. 7. Dependence of the relative output powers at 1062 and 1066 nm on the incident pump power ($\gamma = 1$). Inset: optical spectrum of dual-wavelength operation at the maximum output power.

We rotated the etalon, and adjusted the incident angle θ_i to around 10°, i.e., the ratio of laser thresholds for 1066 and 1062 nm, $\gamma = 1$. Simultaneous laser emission at 1066 and 1062 nm was obtained. Figure 7 shows results on simultaneous dual-wavelength emission at 1062 and 1066 nm. The dual-wavelength laser threshold was 6.7 W. At an incident pump power of 17.6 W, the output power at 1062 nm decreased to 1.3 W and the output power at 1066 nm increased to 1.9 W. A total output power of 3.2 W was achieved with optical conversion efficiency of 18.2%. It can be seen in Fig. 7 that the output powers of both wavelengths linearly increased as the pump power increased. We believe that the competitive interaction between two wavelengths is due to the gain-to-loss balances. The fluctuations for 1062 and 1066 nm lights at the pump power of 17.6 W are about 2.4% and 3.3%, respectively. The spectrum of the dual-wavelength laser at the pump power of 17.6 W is shown in the inset of Fig. 8. The central wavelengths are 1062.4 and 1065.9 nm, with the optical spectral linewidths of 0.38 and 0.35 nm, respectively.

We rotated the etalon, and adjusted the incident angle θ_i to around 30°, i.e., the ratio of laser thresholds for 1066 and

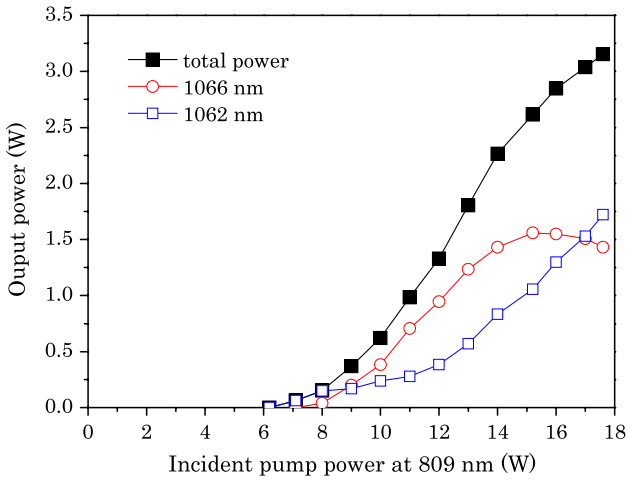

Fig. 8. Dependence of the relative output powers at 1062 and 1066 nm on the incident pump power ($\gamma = 1.1$).

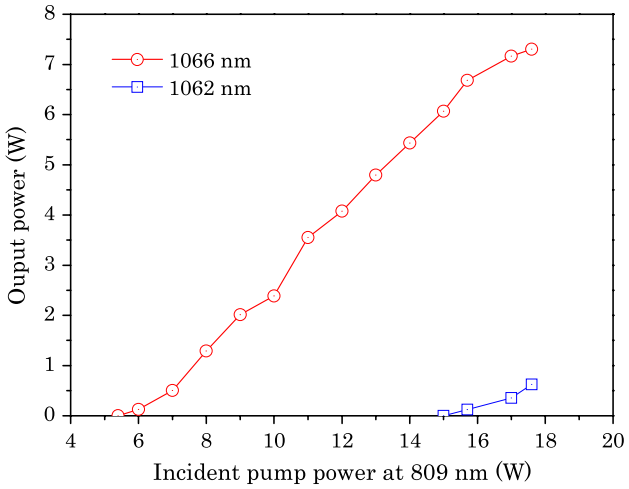

Fig. 9. Dependence of the relative output powers at 1062 and 1066 nm on the incident pump power ($\gamma = 0.95$).

1062 nm, $\gamma = 1.1$. The laser first emits the radiation at the weaker line at 1062 nm. Figure 8 shows results on the dual-wavelength emission at 1062 and 1066 nm. As can be seen from Fig. 8, when $\gamma = 1.1$, the threshold of lasing at 1062 nm was 6.2 W and the output power increased monotonically up to 1.7 W for 17.6 W of pump power. On the other hand, the 1066 nm laser emission started to oscillate at an increased threshold of 7.1 W and reached a maximum output power of 1.6 W at 15.2 W of pump power, with a decrease beyond this pump power.

We adjusted the incident angle θ_i to around 0°, the ratio of laser thresholds for 1066 and 1062 nm, $\gamma = 0.95$. The laser first emits the radiation at the stronger line at 1066 nm. The threshold of lasing at 1066 nm decreased to 5.4 W and the output power increased linearly up to 7.3 W for 17.6 W of pump power. The output powers at each lasing wavelength versus incident power are given in Fig. 9. The 1062 nm laser emission started to oscillate at an increased threshold of 15.6 W and reached a maximum output power of 0.6 W at 17.6 W of pump power. According to the experimental results, as the incident pump power was increased, the 1062 nm transition was not suppressed completely by the 1066 nm transition, but the two wavelength lasing competed with each other.

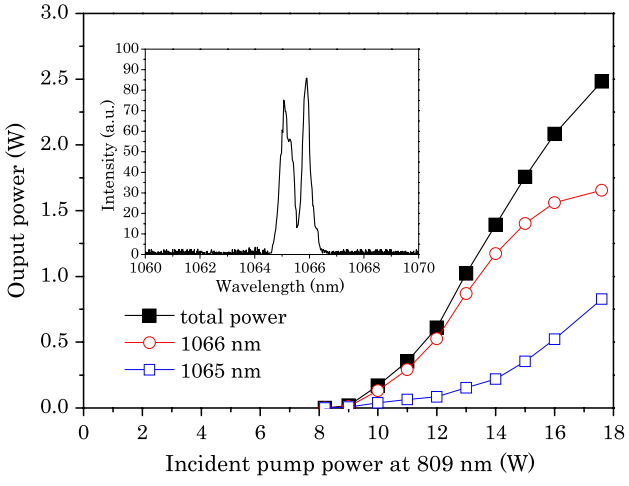

Fig. 10. Dependence of the relative output powers at 1065 and 1066 nm on the incident pump power ($\gamma = 1$). Inset: optical spectrum of dual-wavelength operation at the maximum output power.

We rotated the etalon again, and adjusted the incident angle θ_i to around 40°, i.e., the ratio of laser thresholds for 1066 and 1065 nm, $\gamma = 1$. Simultaneous laser emission at 1065 and 1066 nm was also obtained. The output powers at each lasing wavelength versus incident power are given in Fig. 10. The dual-wavelength laser threshold was 8.2 W. At an incident pump power of 17.6 W, the maximum output power was 0.8 W at 1065 nm and 1.7 W at 1066 nm. A total output power of 2.5 W was achieved with optical conversion efficiency of 14.2%. The spectrum of the dual-wavelength laser at the pump power of 17.6 W is shown in the inset of Fig. 10. The central wavelengths are 1065.1 and 1065.9 nm, with the optical spectral linewidths of 0.46 and 0.34 nm, respectively.

4. CONCLUSION

A diode-end-pumped dual-wavelength Nd:$LuVO_4$ laser with orthogonal polarizations in the range of 1060–1070 nm has been experimentally demonstrated. At 17.6 W of incident pump power, the stable cw simultaneous output power obtained at 1066 and 1068 nm was 3.4 and 2.8 W, respectively. An uncoated glass plane was placed in the π-polarized emission cavity to control the loss of the strong emission, and an etalon was inserted into the σ-polarized emission cavity to select the lasing wavelength of the weak emission. We have theoretically analyzed the condition of gain-to-loss balance for achieving the cw simultaneous dual-wavelength operation. The orthogonally polarized dual-wavelength laser emission was also realized at 1062 and 1066 nm as well as at 1065 and 1066 nm. We believed that the method to control the cavity loss to realize the simultaneous dual-wavelength laser with orthogonal polarizations in this paper can be extended to other polarization-dependent solid-state lasers, such as those with host materials of YVO_4, $GdVO_4$, $YLiF_4$, or $YAlO_3$, for dual-wavelength output.

ACKNOWLEDGMENTS

This work was supported by the National Natural Science Foundation of China (Grants 61108029 and 61275135).

REFERENCES

1. F. Weigl, "A generalized technique of two-wavelength, nondiffuse holographic interferometry," Appl. Opt. **10**, 187–192 (1971).
2. S. N. Son, J. J. Song, J. U. Kang, and C. S. Kim, "Simultaneous second harmonic generation of multiple wavelength laser outputs for medical sensing," Sensors **11**, 6125–6130 (2011).
3. R. W. Farley and P. D. Dao, "Development of an intracavity-summed multiple-wavelength Nd:YAG laser for a rugged, solid-state sodium lidar system," Appl. Opt. **34**, 4269–4273 (1995).
4. Y. F. Chen, Y. S. Chen, and S. W. Tsai, "Diode-pumped Q-switched laser with intracavity sum frequency mixing in periodically poled KTP," Appl. Phys. B **79**, 207–210 (2004).
5. N. G. Basov, M. A. Gubin, V. V. Nikitin, A. V. Nikuchin, V. N. Petrovskii, E. D. Protsenko, and D. A. Tyurikov, "Highly-sensitive method of narrow spectral-line separations, based on the detection of frequency resonances of a 2-mode gas-laser with non-linear absorption," Izv. Akad. Nauk Arm. SSSR, Ser. Fiz.-Mat. Nauk **46**, 1573–1583 (1982).
6. C. G. Bethea, "Megawatt power at 1.318 μ in Nd^{3+}:YAG and simultaneous oscillation at both 1.06 and 1.318 μm," IEEE. J. Quantum Electron. **9**, 254 (1973).
7. K. Gallo and G. Assanto, "All-optical diode based on second-harmonic generation in an asymmetric waveguide," J. Opt. Soc. Am. B **16**, 267–269 (1999).

8. H. Y. Shen, R. R. Zeng, Y. P. Zhou, G. F. Yu, C. H. Huang, Z. D. Zeng, W. J. Zhang, and Q. J. Ye, "Simultaneous multiple wavelength laser action in various neodymium host crystals," IEEE J. Quantum Electron. **27**, 2315–2318 (1991).
9. C. Ren and S. L. Zhang, "Diode-pumped dual-frequency microchip Nd:YAG laser with tunable frequency difference," J. Phys. D **42**, 155107 (2009).
10. Y. Lu, B. G. Zhang, E. B. Li, D. G. Xu, R. Zhou, X. Zhao, F. Ji, T. L. Zhang, P. Wang, and J. Q. Yao, "High power simultaneous dual-wavelength emission of an end-pumped Nd:YAG laser using the quasi-three-level and the four-level transition," Opt. Commun. **262**, 241–245 (2006).
11. N. Pavel, "Simultaneous dual-wavelength emission at 0.90 and 1.06 μm in Nd-doped laser crystals," Laser Phys. **20**, 215–221 (2010).
12. H. Y. Zhu, G. Zhang, C. H. Huang, Y. Wei, L. X. Huang, A. H. Li, and Z. Q. Chen, "1318.8 nm/1338.2 nm simultaneous dual-wavelength Q-switched Nd:YAG laser," Appl. Phys. B **90**, 451–454 (2008).
13. Y. F. Chen, "cw dual-wavelength operation of a diode-end-pumped Nd:YVO_4 laser," Appl. Phys. B **70**, 475–478 (2000).
14. R. Zhou, B. G. Zhang, X. Ding, Z. Q. Cai, W. Q. Wen, P. Wang, and J. Q. Yao, "Continuous- wave operation at 1386 nm in a diode-end-pumped Nd:YVO_4 laser," Opt. Express **13**, 5818–5824 (2005).
15. Y. Y. Lin, S. Y. Chen, A. C. Chiang, R. Y. Tu, and Y. C. Huang, "Single-longitudinal-mode, tunable dual wavelength, CW Nd:YVO_4 laser," Opt. Express **14**, 5329–5334 (2006).
16. R. Zhou, E. B. Li, B. G. Zhang, X. Ding, Z. Q. Cai, W. Q. Wen, P. Wang, and J. Q. Yao, "Simultaneous dual-wavelength CW operation using $^4F_{3/2}$-$^4I_{13/2}$ transitions in Nd:YVO_4 crystal," Opt. Commun. **260**, 641–644 (2006).
17. X. P. Yan, Q. Liu, H. L. Chen, F. Xing, M. L. Gong, and D. S. Wang, "A novel orthogonally linearly polarized Nd:YVO_4 laser," Chin. Phys. B **19**, 084202 (2010).
18. E. Herault, F. Balembois, and P. Georges, "491 nm generation by sum-frequency mixing of diode pumped neodymium lasers," Opt. Express **13**, 5653–5661 (2005).
19. J. L. He, J. Du, J. Sun, S. Liu, Y. X. Fan, H. T. Wang, L. H. Zhang, and Y. Hang, "High efficiency single- and dual-wavelength Nd:$GdVO_4$ lasers pumped by a fiber-coupled diode," Appl. Phys. B **79**, 301–304 (2004).
20. B. Wu, P. P. Jiang, D. Z. Yang, T. Chen, J. Kong, and Y. H. Shen, "Compact dual-wavelength Nd:$GdVO_4$ laser working at 1063 and 1065 nm," Opt. Express **17**, 6004–6009 (2009).
21. K. Lünstedt, N. Pavel, K. Petermann, and G. Huber, "Continuous-wave simultaneous dual-wavelength operation at 912 and 1063 nm in Nd:$GdVO_4$," Appl. Phys. B **86**, 65–70 (2007).
22. Y. F. Chen, M. L. Ku, and K. W. Su, "High-power efficient tunable Nd:$GdVO_4$ laser at 1083 nm," Opt. Lett. **30**, 2107–2109 (2005).
23. Y. P. Huang, C. Y. Cho, Y. J. Huang, and Y. F. Chen, "Orthogonally polarized dual-wavelength Nd:$LuVO_4$ laser at 1086 nm and 1089 nm," Opt. Express **20**, 5644–5651 (2012).
24. H. Y. Shen, R. R. Zeng, Y. P. Zhou, G. F. Yu, C. H. Huang, Z. D. Zeng, W. J. Zhang, and Q. J. Ye, "Comparison of simultaneous multiple wavelength lasing in various neodymium host crystals at transitions from $^4F_{3/2}$-$^4I_{11/2}$ and $^4F_{3/2}$-$^4I_{13/2}$," Appl. Phys. Lett. **56**, 1937–1938 (1990).
25. C. H. Huang, G. Zhang, Y. Wei, L. X. Huang, and H. Y. Zhu, "A Q-switched Nd:$YAlO_3$ laser emitting 1080 and 1342 nm," Opt. Commun. **281**, 3820–3823 (2008).
26. Z. Cong, D. Tang, W. D. Tan, J. Zhang, C. Xu, D. Luo, X. Xu, D. Li, J. Xu, X. Zhang, and Q. Wang, "Dual-wavelength passively mode-locked Nd:$LuYSiO_5$ laser with SESAM," Opt. Express **19**, 3984–3989 (2011).
27. S. Zhuang, D. Li, X. Xu, Z. Wang, H. Yu, J. Xu, L. Chen, Y. Zhao, L. Guo, and X. Xu, "Continuous-wave and actively Q-switched Nd:LSO crystal lasers," Appl. Phys. B **107**, 41–45 (2012).
28. S. D. Liu, L. H. Zheng, J. L. He, J. Xu, X. D. Xu, L. B. Su, K. J. Yang, B. T. Zhang, R. H. Wang, and X. M. Liu, "Passively Q-switched Nd:$Sc_{0.2}Y_{0.8}SiO_5$ dual-wavelength laser with the orthogonally polarized output," Opt. Express **20**, 22448–22453 (2012).
29. L. G. Fei and S. L. Zhang, "The discovery of nanometer fringes in laser self-mixing interference," Opt. Commun. **273**, 226–230 (2007).
30. S. L. Zhang, Y. D. Tan, and Y. Li, "Orthogonally polarized dual frequency lasers and applications in self-sensing metrology," Meas. Sci. Technol. **21**, 054016 (2010).
31. S. Zhang and D. Li, "Using beat frequency lasers to measure micro-displacement and gravity: a discussion," Appl. Opt. **27**, 20–21 (1988).
32. S. Zhang, M. Wu, and G. Jin, "Birefringent tuning double frequency He-Ne laser," Appl. Opt. **29**, 1265–1267 (1990).
33. J. Zhang, T. Feng, S. Zhang, and G. Jin, "Measurements of magnetic fields by a ring laser," Appl. Opt. **31**, 6459–6462 (1992).
34. Y. Ding, S. Zhang, Y. Li, J. Zhu, W. Du, and R. Suo, "Displacement sensors based on feedback effect of orthogonally polarized lights of frequency-split HeNe lasers," Opt. Eng. **42**, 2225–2228 (2003).
35. C. Maunier, J. L. Doualan, R. Moncorgé, A. Speghini, M. Bettinelli, and E. Cavalli, "Growth, spectroscopic characterization, and laser performance of Nd:$LuVO_4$, a new infrared laser material that is suitable for diode pumping," J. Opt. Soc. Am. B **19**, 1794–1800 (2002).
36. W. Shi, Y. J. Ding, N. Fernelius, and K. Vodopyanov, "Efficient, tunable, and coherent 0.18-5.27-THz source based on GaSe crystal," Opt. Lett. **27**, 1454–1456 (2002).
37. J. F. Federici, B. Schulkin, F. Huang, D. Gary, R. Barat, F. Oliveira, and D. Zimdars, "THz imaging and sensing for security applications—explosives, weapons and drugs," Semicond. Sci. Technol. **20**, S266–S280 (2005).
38. J. B. Baxter and G. W. Guglietta, "Terahertz spectroscopy," Anal. Chem. **83**, 4342–4368 (2011).
39. C. B. Reid, E. Pickwell-MacPherson, J. G. Laufer, A. P. Gibson, J. C. Hebden, and V. P. Wallace, "Accuracy and resolution of THz reflection spectroscopy for medical imaging," Phys. Med. Biol. **55**, 4825–4838 (2010).
40. T. Y. Fan and R. L. Byer, "Diode laser-pumped solid-state lasers," IEEE J. Quantum Electron. **24**, 895–912 (1988).
41. D. Findlay and R. A. Clay, "The measurement of internal losses in 4-level lasers," Phys. Lett. **20**, 277–278 (1966).
42. M. Born and E. Wolf, *Principles of Optics: Electromagnetic Theory of Propagation, Interference and Diffraction of Light*, 7th (expanded) ed. (Cambridge University, 1999).